Available online at www.sciencedirect.com
ScienceDirect
Biochemical and Biophysical Research Communications 351 (2006) 223–228
BBRC
www.elsevier.com/locate/ybbrc

Recombinant amyloidogenic domain of ApoA-I: Analysis of its fibrillogenic potential ☆

Sonia Di Gaetano [a], Fulvio Guglielmi [b], Angela Arciello [b], Palma Mangione [c], Maria Monti [d,e], Daniela Pagnozzi [d], Sara Raimondi [c], Sofia Giorgetti [c,f], Stefania Orrù [d], Claudio Canale [g], Piero Pucci [d,e], Christopher M. Dobson [h], Vittorio Bellotti [c,f], Renata Piccoli [b,*]

[a] *Istituto di Biostrutture e Bioimmagini, CNR, Napoli 80134, Italy*
[b] *Dipartimento di Biologia Strutturale e Funzionale, Università di Napoli Federico II, Complesso Universitario di Monte S. Angelo, via Cinthia 4, Napoli 80126, Italy*
[c] *Dipartimento di Biochimica, Università di Pavia, Pavia 27100, Italy*
[d] *CEINGE Biotecnologie Avanzate, Napoli 80131, Italy*
[e] *Dipartimento di Chimica Organica e Biochimica, Università di Napoli Federico II, Napoli 80126, Italy*
[f] *Laboratorio di Biotecnologie IRCCS, Pavia 27100, Italy*
[g] *Dipartimento di Fisica, Università di Genova, Genova 16146, Italy*
[h] *Department of Chemistry, University of Cambridge, Cambridge CB2 IEW, UK*

Received 3 October 2006
Available online 23 October 2006

Abstract

A variety of amyloid diseases are associated with fibrillar aggregates from N-terminal fragments of ApoA-I generated through a largely unexplored multi-step process. The understanding of the molecular mechanism is impaired by the lack of suitable amounts of the fibrillogenic polypeptides that could not be produced by recombinant methods so far. We report the production and the conformational analysis of recombinant ApoA-I 1–93 fragment. Similarly to the polypeptide isolated *ex vivo*, a pH switch from 7 to 4 induces a fast and reversible conformational transition to a helical state and leads to the identification of a key intermediate in the fibrillogenesis process. Limited proteolysis experiments suggested that the C-terminal region is involved in helix formation. The recombinant polypeptide generates fibrils at pH 4 on a time scale comparable with that of the native fragment. These findings open the way to studies on structural, thermodynamic, and kinetic aspects of ApoA-I fibrillogenesis.

Keywords: Fibrillogenesis; ApoA-I amyloidosis; Recombinant amyloidogenic proteins; Conformational analysis

Abnormal conformations of specific proteins and polypeptides represent the underlying pathogenic basis of amyloid diseases [1]. A variety of amyloid diseases are associated with mutations in apolipoprotein A-I (ApoA-I), for which the process of fibril formation has not yet been clarified, and a paucity of information exists in comparison to the detailed knowledge surrounding other disease-associated proteins such as lysozyme, transthyretin, and β2-microglobulin [1]. Analysis of natural amyloid fibrils has shown that fibrils consist of ApoA-I N-terminal fragments, 90–100 residues long. Mutations are sometimes present within the N-terminal portion of the protein that is

☆ *Abbreviations:* AFM, atomic force microscopy; ApoA-I, apolipoprotein A-I; [1–93]ApoA-I, the 93-residues N-terminal domain of ApoA-I; ANS, 8-anilino-1-naphthalenesulphonate; DTT, dithiothreitol; TEM, transmission electron microscopy; ESMS, electrospray mass spectrometry; IPTG, isopropyl-β-D-thiogalactopyranoside; MALDI-MS, matrix assisted laser desorption ionization mass spectrometry; TFE, trifluoroethanol.

* Corresponding author. Fax: +39 081 679233.
E-mail address: piccoli@unina.it (R. Piccoli).

0006-291X/$ - see front matter © 2006 Elsevier Inc. All rights reserved.
doi:10.1016/j.bbrc.2006.10.026

eventually found in fibrils (''internal mutations''), but can also occur in positions located outside this region of the polypeptide sequence (''external mutations'') [2].

Characterization of the polypeptides purified from natural fibrils from patients carrying the ''external mutation'' Leu174Ser has shown that the 1–93 N-terminal portion of ApoA-I is intrinsically amyloidogenic in a physiological environment. By using the natural 1–93 polypeptide, we have shown that acidic conditions (pH 4) induce fibril formation [3]. We envisage a complex aggregation pathway in which the polypeptide assumes a random coil structure at neutral pH, shifts into an unstable helical conformation at acidic pH, and then aggregates into a β-sheet-based polymeric structure. The investigation of this complex pathway has been limited so far by the small amounts of the natural amyloidogenic polypeptide. Attempts to express an homologous recombinant form either in prokaryotic or eukaryotic cells have failed, probably for the rapid intracellular digestion of the unstructured product.

We describe here the production of recombinant 1–93 polypeptide and the investigation of its structural dynamics during fibrillogenesis.

Materials and methods

Expression and isolation of Apo A-I 1–93 polypeptide. The cDNA encoding fragment 1–93 of ApoA-I ([1–93]ApoA-I) was obtained by PCR amplification using full length ApoA-I cDNA as a template, and oligonucleotides 5′-CGCGGATCCGATGAACCCCCCCAGAG-3′ (forward primer) and 5′-CCGGAATTCTTACACCTCCTCCAGATCCTTG-3′ (reverse primer), where restriction sites are underlined. The amplified DNA was cloned in the *Eco*RI and *Bam*HI sites of pGEX-4T-3 expression vector (General Electric, CT) downstream to the sequence encoding glutathione *S*-transferase (GST). Competent *Escherichia coli* BL21DE3 cells were transformed and induced to express the recombinant protein by the addition of 0.1 mM IPTG for 2 h at 37 °C, using a BioFlo 3000 benchtop fermentor (New Brunswick Scientific, NY).

Isolation of recombinant [1–93]ApoA-I. Lysates were obtained upon treatment of bacteria with 1% Triton X-100 in PBS (30 min, 4 °C) in the presence of protease inhibitors (Roche, Germany), followed by sonication (Misonix, Farmingdale, NY). The soluble fraction obtained by centrifugation was fractionated by affinity chromatography on a GSTrap glutathione-agarose column. GST-containing species were eluted with 50 mM Tris–HCl at pH 8.0, containing 10 mM glutathione following the manufacturer's protocol, but in the absence of DTT to avoid inhibition of thrombin enzymatic activity. Proteins were then digested with 6 U/mg of thrombin (Sigma) for 30 h at 4 °C in the chromatography elution buffer. Products were separated by HPLC reverse chromatography on a Ultrapure C_8 column (Beckman Coulter, CA) with a linear gradient of acetonitrile in 5 mM phosphate buffer at pH 7.4 and analysed by SDS–PAGE on 15% acrylamide gels. For Western blot analyses anti-human ApoA-I polyclonal antibodies (DAKO, Denmark) and a chemiluminescence detection system (West Pico, Pierce) were used. Pure [1–93]ApoA-I was dialyzed in water, lyophilized, and stored at −70 °C until use. The lyophilized polypeptide was dissolved in phosphate buffer at pH 7.4. About 1 mg of pure [1–93]ApoA-I was obtained from 1 L of bacterial culture.

In situ hydrolysis and MALDI-MS analysis. The protein band stained by Coomassie blue brilliant and corresponding to the expected recombinant protein was excised and *in situ* digested according to [4] and the peptide mixture was analysed by MALDI as described [5].

Limited proteolysis. Aliquots of 7 μM [1–93]ApoA-I were digested separately with trypsin, V8 protease, chymotrypsin, elastase, and subtilisin. Proteolysis was performed at 25 °C in 12 mM sodium phosphate at pH 7.5, using enzyme-to-substrate ratios ranging between 1:800 and 1:4000 (w/w). Proteolysis in the presence of 20% TFE was performed under the same conditions using enzyme-to-substrate ratios ranging from 1:100 to 1:2000 (w/w). The extent of proteolysis was monitored by sampling the incubation mixture at different time intervals. Proteolytic fragments were fractionated and characterized by mass spectrometry as described [5].

Gel-filtration assay. Gel-filtration experiments were performed with a SMART system (Pharmacia Biotech) using a Superdex-75 column (Pharmacia) equilibrated and eluted in 50 mM phosphate buffer at pH 7.5, containing 150 mM NaCl, in the presence or absence of 20% TFE. [1–93]ApoA-I (4 μg) was dissolved in an appropriate volume of buffer with or without TFE (20%) to a final concentration of 7 μM. Experiments were performed at room temperature at a flow rate of 75 μl/min. The column was calibrated under the same conditions (either with or without 20% TFE) with standard proteins.

CD spectra. Circular dichroism spectra were recorded on a Jasco J-710 spectropolarimeter as previously described [3]. Measurements were performed at 20 °C at a protein concentration of 0.3 mg/ml in 3 mM glycine, 3 mM sodium acetate, and 3 mM sodium phosphate at pH 7 (buffer A). Acidification and neutralization of the solution were carried out as previously described [3]. CD data were expressed as mean residue ellipticity (θ).

Fluorescence spectra at the equilibrium. By observing the intrinsic fluorescence emission of tryptophan in the range 300–550 nm and excitation at 295 nm, we monitored the conformational transition induced by the pH jump from 7 to 4. Measurements were carried out at 20 °C in a 10-mm cell by using a Perkin-Elmer LS50 spectrofluorimeter and the slit widths set at 5 nm. Protein solution (0.06 mg/ml) was first analysed in buffer A (see above). The solution was then analysed after acidification to pH 4 followed by neutralization to pH 7 by adding HCl and NaOH, respectively, to give a concentration of 3.8 mM in each sample.

Stopped-flow fluorescence spectra. The kinetics of the [1–93]ApoA-I structural transition from pH 7 to pH 4 were monitored at 20 °C on a Bio-Logic SFM-300 stopped flow fluorimeter using an excitation wavelength of 295 nm and monitoring the total fluorescence emission change over 320 nm. One volume of 0.6 mg/ml peptide solution in buffer A (see above) was mixed with five volumes of 5.4 mM glycine, 5.4 mM sodium acetate, and 5.4 mM sodium phosphate at pH 7, and four volumes of 0.01 N HCl.

Binding to 8-anilino-1-naphthalenesulphonate (ANS). ANS binding experiments were carried out on solutions containing [1–93]ApoA-I (2.8 μM) and ANS (330 μM) in buffer A (see above). 8-Anilino-1-naphthalenesulphonate emission fluorescence spectra were recorded in the range 400–600 nm at an excitation wavelength of 395 nm and the slit widths set at 5 nm [6]. Spectra were then recorded after acidification to pH 4, and then after returning to pH 7.

Fibrils imaging. Samples for TEM were prepared by floating the aggregate suspension on formvar/carbon-coated grids for 2–3 min, before air-drying and staining them with 2% uranyl acetate. Samples were examined in a Jeol JEM 1200 EX electron microscope operating at 180 kV. For AFM imaging, [1–93]ApoA-I solution (0.25 mg/ml) was incubated at pH 4 and 25 °C for two weeks and analysed as previously described [7].

Results

Expression and isolation of recombinant [1–93]ApoA-I as a stable product

The 1–93 fragment of ApoA-I was expressed in bacterial cells following an experimental strategy aimed at reducing the intracellular degradation of the polypeptide during its production. It was expressed as a chimeric protein obtained by fusing the 93 residues polypeptide to glutathione

S-transferase (GST). Analyses by SDS–PAGE of bacterial lysates showed the presence of a major protein species in IPTG-induced cells (Fig. 1A, lane 3) with a molecular mass of about 36 kDa, as expected for the chimeric product, and specifically recognised by an anti-ApoA-I antibody (Fig. 1B, lane 3). In this sample, additional immunopositive species with a molecular mass lower than that of the chimeric protein were also present (see below).

GST-containing proteins, selected on a GSH-agarose affinity column, were analysed by SDS–PAGE (Fig. 1A, lane 4) and found to contain exclusively species recognized by the anti-ApoA-I antibody (Fig. 1B, lane 4). Coomassie-stained protein bands corresponding to these immunopositive species were excised from the gel and digested *in situ* with trypsin. The resulting peptide mixtures were directly analysed by MALDI mass spectrometry. Mass signals were mapped onto the anticipated ApoA-I sequence and showed that the main product was the GST-[1–93]ApoA-I full length chimeric protein (indicated in Fig. 1 by an arrow). In addition to this product, small quantities of C-terminal truncated [1–93]ApoA-I species were also identified.

The [1–93]ApoA-I moiety was released from the chimeric protein by targeted proteolysis, making use of a unique cleavage site for thrombin positioned between the GST and the [1–93]ApoA-I coding sequences. The proteolysis mixture, analysed by SDS–PAGE and Western blot (Fig. 1A and B, lane 5), was resolved by reverse-phase HPLC. The major eluted fraction was found to contain a pure protein species with the same electrophoretic mobility as the native fibrillogenic polypeptide [8] recognized by the anti-ApoA-I antibody (Fig. 1A and B, lane 6). An aliquot of this protein was analysed by electrospray mass spectrometry (ESMS) showing a molecular mass of 10863.8 ± 0.1 Da, perfectly matching the expected mass value of [1–93]ApoA-I with the extra dipeptide Gly-Ser at the N-terminus originating from the plasmid construct following thrombin cleavage (10864.0 Da).

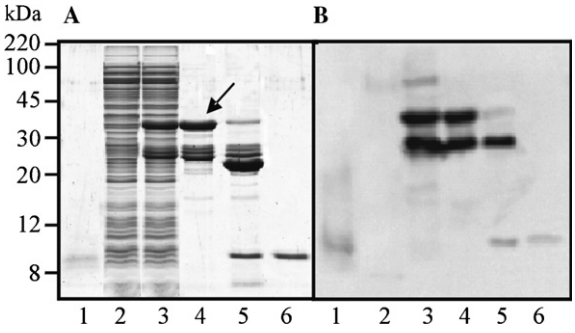

Fig. 1. Analysis by SDS–PAGE of recombinant [1–93]ApoA-I. (A) Coomassie staining; (B) Western blotting. Lane 1, native [1–93]ApoA-I extracted from *ex vivo* fibrils; lanes 2 and 3, soluble fractions prepared from non-induced cells (lane 2) or induced cells (lane 3); lane 4, GST-containing proteins selected by affinity chromatography; lane 5, thrombin proteolytic products; lane 6, HPLC purified [1–93]ApoA-I. The arrow indicates the full length GST-fused [1–93]ApoA-I.

CD spectroscopic analysis

The overall far UV CD spectrum of [1–93]ApoA-I at neutral pH (Fig. 2A), with a minimum at 203 nm, indicates that the peptide is highly unstructured under these conditions. A marked change in the spectrum is observed at pH 4, with the major minimum in the spectrum shifting from 203 to 208 nm and a considerable increase in ellipticity at 222 and 190 nm. Such spectral changes are consistent with a transition to helical structure at pH 4, and are in good agreement with the behaviour of the natural [1–93]ApoA-I polypeptide [3]. In a similar way, we have previously described the decay of the CD signal associated with protein aggregation and precipitation as well as the progressive loss of CD signal and the further aggregation when the protein is left at pH 4 [3]. The pH-induced changes in the spectrum can be reversed if NaOH is added within a few seconds to neutralize the pH (Fig. 2A). Fig. 2B reports the time dependence of CD spectra changes of [1–93]ApoA-I upon exposure to acidic conditions. After 60 min of incubation at pH 4 the spectra show the disappearance of the minimum at 222 and the persistence of a second minimum at 205 nm that is suggestive of a transition to β-sheet structure.

Fluorescence spectroscopy

Tryptophan emission fluorescence was monitored for [1–93]ApoA-I at pH 7 and 4 (Fig. 2C). A blue shift from 347 to 342 nm occurs during the pH transition and is associated with a decrease in the fluorescence intensity in complete agreement with the data obtained for the natural peptide [3]. The effect of the pH jump on the intrinsic fluorescence spectrum is consistent with the collapse of the protein core region and the exclusion of water molecules in the vicinity of aromatic residues. This transition again is fully reversible when the pH is rapidly returned to 7. The rate of the conformational transition induced by low pH was then investigated by monitoring the change in the tryptophan intrinsic fluorescence under stopped flow conditions (inset of Fig. 2C). The 5% decrease of intrinsic fluorescence emission, expected on the basis of studies carried at the equilibrium, is complete in approximately 2 s ($k = 1.01\ s^{-1}$) and 90% of this change takes place within the lag time of the data acquisition (<2 ms).

ANS binding

The binding of the apolar dye ANS to [1–93]ApoA-I is associated with an enhanced fluorescence intensity and a blue shift in the emission wavelength. Such changes are frequently used to detect partially folded intermediate states of globular proteins and are characteristic of solvent-exposed hydrophobic clusters [9]. In the case of [1–93]ApoA-I, binding of ANS to the protein at pH 7 leads to a slight blue shift from 515 to 489 nm but no increase in fluorescence emission (compare Fig. 2D with inset).

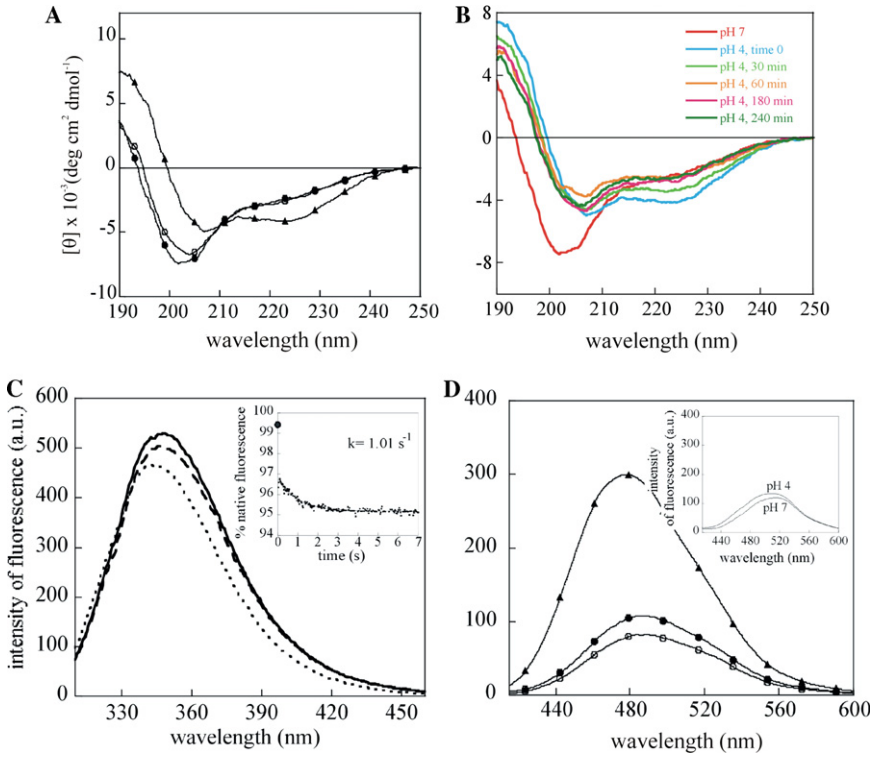

Fig. 2. Spectroscopic analyses of [1–93]ApoA-I. (A) pH-induced transition of [1–93]ApoA-I secondary structure monitored by far UV CD. Spectra were recorded at pH 7 (●), pH 4 (▲), and then returned to pH 7 (○). (B) Time dependence of the induction of secondary structure of [1–93]ApoA-I at pH 4. The far UV CD spectra were recorded at pH 7 and after a pH jump to pH 4 at the indicated time intervals. (C) Effect of pH on the intrinsic fluorescence of [1–93]ApoA-I. Tryptophan emission was monitored at pH 7 (solid line), after a pH jump to 4 (dotted line), and then a return to pH 7 (dashed line). The inset shows the rate of change of intrinsic fluorescence acquired during the pH jump. The data were normalized by defining the fluorescence of the protein at pH 7 as 100%. The continuous line through the data points represents the best fit to a single exponential function. The symbol on the abscissa refers to the fluorescence intensity recorded at $t = 0$. (D) pH-induced binding of ANS to [1–93]ApoA-I. Symbols are as (A). ANS emission fluorescence spectra were recorded in the range of 400–600 nm at the excitation wavelength of 395 nm with the slit widths set at 5 nm. Spectra of the free dye at pH 7 and 4 are shown in the inset.

Reduction in the pH, however, leads to a substantial change of ANS fluorescence reflecting the pH-induced transformation into a partially folded conformation; at pH 4 the ANS maximum emission shifts to 477 nm with a considerable increase in fluorescence intensity (Fig. 2D) consistent with the behaviour previously ascribed to proteins in a molten globule state [9].

The ANS–[1–93]ApoA-I complex at pH 4 dissociates when the pH is returned to pH 7 and this reversibility is consistent with data derived from the CD and intrinsic fluorescence spectra. The pH dependence of the fluorescence intensity of the free dye is shown for comparison in the inset of Fig. 2D.

Limited proteolysis

The conformational transitions of [1–93]ApoA-I were investigated by limited proteolysis coupled with mass spectrometry both in the presence and in the absence of TFE (20% at pH 7.5), which induces a stable helical state. The patterns of preferential proteolytic sites were obtained using a set of five proteases (trypsin, V8 protease, chymotrypsin, elastase, and subtilisin) as conformational probes [5]. For each protease, the appropriate enzyme/protein ratio was carefully determined to generate a limited number of proteolytic events directed to the most flexible and solvent-exposed regions of the polypeptide chain. Proteolytic fragments were separated by reverse-phase HPLC and identified by ESMS, allowing the positions of the cleavage sites to be assigned.

Fig. 3A summarizes the overall data from limited proteolysis experiments. In the absence of TFE, the polypeptide chain is preferentially cleaved in its central region, between residues 17 and 61, whereas the N-terminal region (residues 1–16) and the large segment 62–93 at the C-terminus are protected. Similar results were obtained when the proteolysis experiments were carried out in the presence of 20% TFE.

Gel filtration

The oligomeric state of the amyloidogenic [1–93]ApoA-I fragment was assessed by gel-filtration chromatography at pH 7.5 both in the presence and in the absence of 20% TFE. Interestingly, under native conditions the elution volume of [1–93]ApoA-I species was consistent with a dimeric

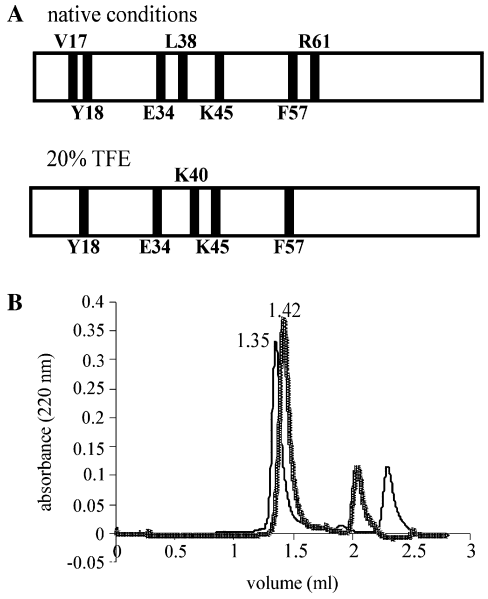

Fig. 3. (A) Schematic representation of the results obtained by limited proteolysis experiments. Preferential proteolytic sites occurring in [1–93]ApoA-I in the absence (native conditions) and presence of 20% TFE are indicated by solid bars. (B) Investigation of the oligomeric state of [1–93]ApoA-I by gel-filtration chromatography, in the absence (thin line) or presence (heavy line) of 20% TFE. The corresponding elution volumes are indicated.

structure, whereas in the presence of the co-solvent the protein showed the behaviour of a monomeric species (Fig. 3B).

Fibril formation

The formation of amyloid fibrils at pH 4 was monitored by electron microscopy and atomic force microscopy. Fig. 4A shows an electron microscopy image of a fibrils nest obtained with recombinant [1–93]ApoA-I. Images obtained by AFM are presented in Fig. 4B. Narrow protofilaments and well-defined fibrils were detectable after 72–90 h of incubation at pH 4, consistent with the rate observed for the native protein [3]. Fibrillar structures coexist with globular aggregates whose height is between 4 and 10 nm. The heights of protofilaments and mature fibrils are 0.8 ± 0.3 nm and 2.4 ± 0.6, values in agreement with those measured by tapping mode AFM in air for *ex vivo* amyloid fibrils formed by Leu174Ser ApoA-I [7]. The relatively small height values measured by AFM in air are associated with sample drying, which results in dehydration and possibly deformation of the fibrils upon adhesion to the mica substrate. On the other hand, for Leu174Ser ApoA-I fibrils, a diameter of about 7 nm was estimated by electron microscopy [10] and a height value of 11 nm was measured by AFM under fully hydrated conditions [7].

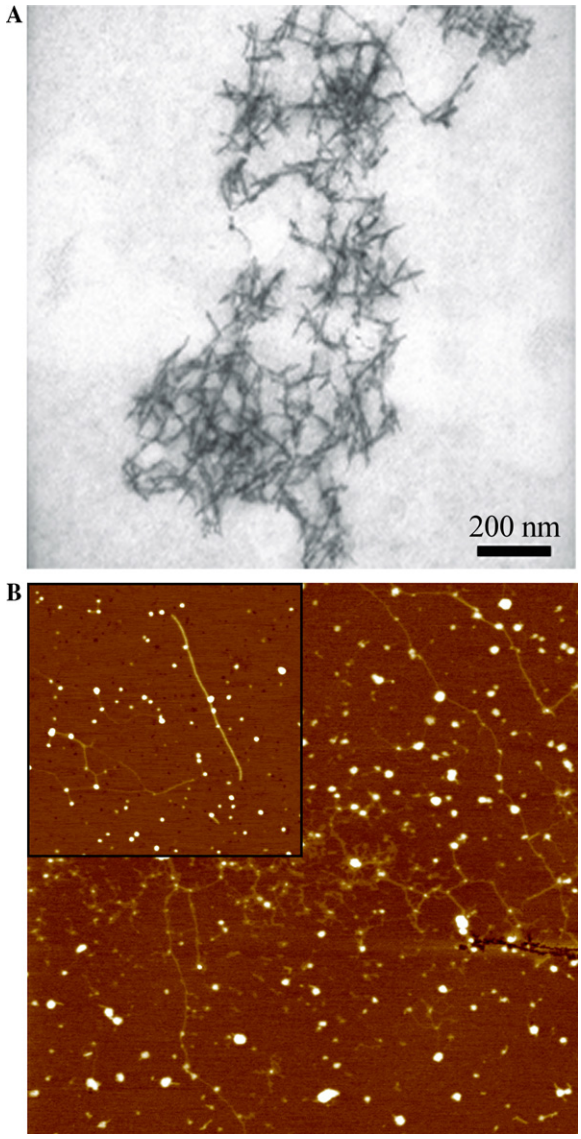

Fig. 4. Microscopic analyses of aggregated [1–93]ApoA-I. (A) Transmisson electron microscopy image of [1–93]ApoA-I fibrils stained by 2% uranyl acetate. (B) Tapping mode atomic force microscopy image of [1–93]ApoA-I fibrillar material showing a network of thin filaments coexisting with globular aggregates. Scan size, 4.0 μm; *Z* range, 15 nm. Inset, thin filaments and a fibril approximately 1 μm long. Globular aggregates are also present. Scan size, 1.8 μm; *Z* range, 10 nm.

Discussion

In the present study an efficient strategy to produce a recombinant version of the 1–93 amyloidogenic domain of ApoA-I has been established. The investigation of the conformation of this polypeptide in solution indicates that in physiological conditions the protein has a highly unfolded structure. A decrease in the pH value from 7 to 4 induces a predominant α-helical structure, by inducing the conversion of the protein from a random coil to a helical/molten globule state, capable to bind ANS. This transition, complete within 2 s and fully reversible when the pH is returned to 7, is followed by the appearance of a significant β-sheet component. The helical/molten globule intermediate displays a strong propensity to oligomerize; indeed attempts to analyse this intermediate by gel-filtration failed due to the rapid formation of insoluble species (data not shown).

The conformation of [1–93]ApoA-I polypeptide in the helical state was further investigated by stimulating the helical conformation at neutral pH by treatment with 20% trifluoroethanol [11]. Limited proteolysis experiments, performed both in the absence and in the presence of the co-solvent, indicated a nearly identical distribution of preferential proteolytic sites, with the C-terminal region of the polypeptide chain being inaccessible to proteases in both conditions. Gel-filtration suggests that [1–93]ApoA-I, while dimeric in native conditions, is monomeric in the presence of TFE. The inaccessibility of the C-terminus in native conditions might then be a consequence of the dimeric structure of the polypeptide, whereas the local stabilization induced by TFE makes this region resistant to proteolytic attack in the monomeric form.

Analyses by electron and atomic force microscopy have demonstrated that [1–93]ApoA-I generates typical amyloid fibrils following incubation at pH 4 for lengths of time comparable to those required by the natural counterpart.

Our results on recombinant [1–93]ApoA-I confirm and expand the data obtained with its natural counterpart and focus our attention on the kinetics and stability of the helical/molten globule state, as a key intermediate in the multistep fibrillogenic process. These findings also encourage the production of the variants of this polypeptide described in patients affected by ApoA-I associated amiloidoses. A detailed comparative study on the conformational dynamics and fibrillogenic potential of mutated forms versus wild type [1–93]ApoA-I would contribute greatly to the comprehension of the molecular mechanism by which mutations in ApoA-I promote amyloid deposition.

Acknowledgments

This study was supported by MIUR, Ministero dell'Università e della Ricerca Scientifica (PRIN 2005053998, FIRB 2001 project RBNE01S29H, and FIRB 2001 project RBAU015B47). Ricerca finalizzata Ministero della Salute, Fondazione Cariplo (Progetto Nobel), and by Regione Campania (2002). The research of C.M.D. is supported by Programme Grants from the Wellcome and Leverhulme Trusts.

References

[1] F. Chiti, C.M. Dobson, Protein misfolding, functional amyloid, and human disease, Annu. Rev. Biochem. 75 (2006) 333–366.
[2] L. Obici, G. Franceschini, L. Calabresi, S. Giorgetti, M. Stoppini, G. Merlini, V. Bellotti, Structure, function and amyloidogenic propensity of apolipoprotein A-I, Amyloid 13 (2006) 1–15.
[3] A. Andreola, V. Bellotti, S. Giorgetti, P. Mangione, L. Obici, M. Stoppini, J. Torres, E. Monzani, G. Merlini, M. Sunde, Conformational switching and fibrillogenesis in the amyloidogenic fragment of apolipoprotein A-I, J. Biol. Chem. 278 (2003) 2444–2451.
[4] A. Shevchenko, P. Keller, P. Scheiffele, M. Mann, K. Simons, Identification of components of *trans*-Golgi network-derived transport vesicles and detergent-insoluble complexes by nanoelectrospray tandem mass spectrometry, Electrophoresis 18 (1997) 2591–2600.
[5] A. Scaloni, N. Miraglia, S. Orru, P. Amodeo, A. Motta, G. Marino, P. Pucci, Topology of the calmodulin-melittin complex, J. Mol. Biol. 277 (1998) 945–958.
[6] D.P. Rogers, C.G. Brouillette, J.A. Engler, S.W. Tendian, L. Roberts, V.K. Mishra, G.M. Anantharamaiah, S. Lund-Katz, M.C. Phillips, M.J. Ray, Truncation of the amino terminus of human apolipoprotein A-I substantially alters only the lipid-free conformation, Biochemistry 36 (1997) 288–300.
[7] A. Relini, R. Rolandi, M. Bolognesi, A. Gliozzi, M. Aboudan, G. Merlini, V. Bellotti, Ultrastructural organization of ex-vivo amyloid fibrils formed by the apolipoprotein A-I Leu174Ser variant: an atomic force microscopy study, Biochim. Biophys. Acta 1690 (2004) 33–41.
[8] L. Obici, V. Bellotti, P. Mangione, M. Stoppini, E. Arbustini, R. Verga, I. Zorzoli, E. Anesi, G. Zanotti, C. Campana, M. Viganò, G. Merlini, The new apolipoprotein A-I variant $Leu^{174} \rightarrow Ser$ causes chardiac amyloidosis, and the fibrils are constituted by the 93-residue N-terminal polypeptide, Am. J. Pathol. 155 (1999) 695–702.
[9] G.V. Semisotnov, N.A. Rodinova, O.I. Razgulyaev, V.N. Uversky, A.F. Gripas, R.I. Gilmanshin, Study of the "molten globule" intermediate state in protein folding by a hydrophobic fluorescent probe, Biopolymers 31 (1991) 119–128.
[10] P. Mangione, M. Sunde, S. Giorgetti, M. Stoppini, G. Esposito, L. Gianelli, L. Obici, L. Asti, A. Andreola, P. Viglino, G. Merlini, V. Bellotti, Amyloid fibrils derived from the apolipoprotein A-I Leu174Ser variant contain elements of ordered helical structure, Protein Sci. 10 (2001) 187–199.
[11] M. Buck, Trifluoroethanol and colleagues: cosolvents come of age. Recent studies with peptides and proteins, Q. Rev. Biophys. 31 (1998) 297–355.